Optical electron polarimetry with heavy noble gases

T. J. Gay,* J. E. Furst,† K. W. Trantham,* and W. M. K. P. Wijayaratna‡
Department of Physics, University of Missouri-Rolla, Rolla, Missouri 65401
(Received 26 June 1995)

We have measured the polarization of fluorescence emitted by the noble gases He, Ne, Ar, Kr, and Xe following impact excitation by polarized electrons. In He, the $3^3P \rightarrow 2^3S$ transition was studied; in the heavy noble gases the $np^5(n+1)p\ ^3D_3 \rightarrow np^5(n+1)s\ ^3P_2$ transitions were analyzed. We investigated these transitions as candidates for efficient optical electron polarimetry and found that, because of their larger excitation cross sections and analyzing power, the heavy noble gases are superior to He, which had been used previously as a polarimetric target. Several issues with regard to the implementation and accuracy of optical electron polarimetric techniques are discussed.

PACS number(s): 34.80.Dp, 07.60.Fs, 07.90.tc, 34.80.Nz

I. INTRODUCTION

Although the idea of optical electron polarimetry was discussed as early as 1956 [1], the first detailed proposals for such a technique were made by Farago and Wykes more than a decade later [2]. Optical schemes have a number of attractive features when compared with traditional Mott polarimetry. Not requiring high voltage, they are relatively easy to implement, have good analyzing power, and have the potential to provide an absolute polarimetric standard without requiring calibration or resort to dynamical theoretical calculation. The Farago and Wykes proposals involved the impact excitation of group-IIB targets (Zn, Cd, Hg) by electrons whose polarization was to be determined, with measurement of the circular polarization of the subsequent fluorescence. The first demonstration of the optical method was made by Eminyan and Lampel in 1980, using a zinc target [3]. Wolcke *et al.* used mercury in a similar fashion three years later [4].

Subsequently, Gay proposed the use of He instead of the group-IIB elements [5]. Helium has some significant advantages for polarimetry, the two most important being its practicality as an electron scattering target and its realization of the original hope of Farago and Wykes for a polarimetric technique not requiring calibration. A He polarimeter was first demonstrated at Münster [6], and has since been used in a number of other laboratories [7,8].

In a standard optical measurement, photons produced by polarized electron-impact excitation are observed along the direction of the initial polarization vector (e.g., $P\hat{y}$; see Fig. 1). The scattered electrons are not detected. In this case, a generic polarimeter equation may be written [9] involving P:

$$\eta_2 = \gamma P(1+\beta\eta_3) \equiv AP. \tag{1}$$

Here γ and β are constants that depend on the atomic target and the specific optical transition used and are, ideally, independent of the incident electron energy E. The quantity A is usually referred to as the polarimeter's "analyzing power." The relative Stokes parameters η_2 and η_3 are the circular and linear polarization of the light, respectively, the latter being associated with the incident electron-beam direction (e.g., $\hat{z}$) and $\hat{x}$. (The third Stokes parameter η_1 is the linear polarization in the xz plane corresponding to axes at 45° and 135° relative to $\hat{z}$, and will be considered below.) The value of η_3 corresponds to the second moment of electron density along $\hat{z}$ (alignment), and generally depends on E.

The values of γ and β may depend on E for two reasons. If the electron beam has sufficient energy to excite states that lie above the initial state i of the relevant optical transition, they may decay into i at a rate that varies with their population, and hence with E. Alternatively, if the total orbital angular momentum L and spin angular momentum S of the collision complex are not conserved separately during the collision, or if i is not a well-LS-coupled state, γ and β will generally exhibit an energy dependence [10,11]. The former situation can occur when significant spin-orbit forces act on the continuum electron (Mott scattering), or when a temporary negative ion is formed during the collision. Negative ion resonances also affect η_3 [5]. When all of the above effects

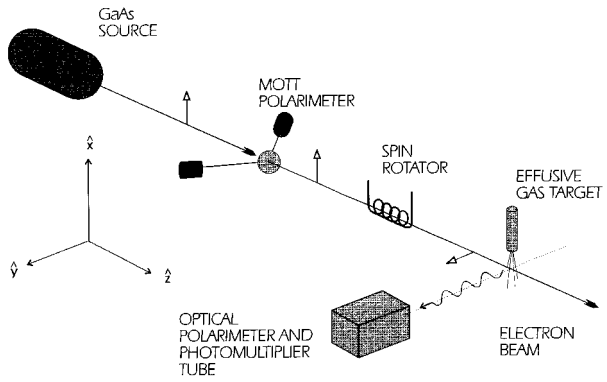

FIG. 1. Schematic diagram of the experimental apparatus with the coordinate system used in the text. Open arrows indicate electron polarization vectors.

*Present address: Behlen Laboratory of Physics, University of Nebraska, Lincoln, Nebraska 68588-0111 (address to which correspondence should be sent).

†Present address: Department of Physics, Central Coast Campus, University of Newcastle, Ourimbah NSW 2258, Australia.

‡Present address: Department of Physics, University of Colombo, Colombo 03, Sri Lanka.

 © 1996 The American Physical Society

TABLE I. Polarimetric transitions for the noble gases (see text). Values of γ, β, and A (threshold) are taken from Refs. [5] and [9].

Target	Transition	E_t (eV)	E_c (eV)	First cascading state	σ_{max} (10^{-19} cm^2)	γ	β	A (threshold)
He	$3\,^3P \rightarrow 2\,^3S$ (3889 Å)	23.00	23.59	$4\,^3S$[a]	7.0 (Ref. [13])	0.5000	−0.3333	0.4390
Ne	$3\,^3D_3 \rightarrow 2\,^3P_2$ (6402 Å)	18.55	19.66	$4\,^3P_2^o$	91 (Ref. [14])	0.6663	0.2230	0.7315
Ar	$4\,^3D_3 \rightarrow 3\,^3P_2$ (8115 Å)	13.07	13.90	$3d_3$	260 (Ref. [15])	0.6667	0.2222	0.7317
Kr	$5\,^3D_3 \rightarrow 4\,^3P_2$ (8112 Å)	11.44	12.11	$3d_3$	120[b] (Ref. [16])	0.6214	0.2768	0.6959
Xe	$6\,^3D_3 \rightarrow 5\,^3P_2$ (8819 Å)	9.72	9.94	$5\,^3F_4^o$	280[b] (Ref. [16])	0.6322	0.3098	0.7080

[a]The $3\,^3D$ state decays almost exclusively to the $2\,^3P$ state (see text).
[b]Extrapolated to zero target pressure.

are negligible, γ and β can be calculated using angular momentum coupling algebra only, and thus P can be extracted directly from Eq. (1) without the need for a calibration measurement. This is the case with He when E is in the range from 23.0 eV, the excitation threshold of i, the $3\,^3P$ state, to 23.6 eV, the threshold for the $4\,^3S$ state, the first important upper cascading level. (The $3\,^3P$ to $2\,^3P$ branching ratio for decay of the $3\,^3D$ state is 1.8×10^{-4} [12].)

The elegance of optical electron polarimetry is this: by measuring the three relative Stokes parameters η_1, η_2, and η_3, one determines P and, simultaneously, characterizes the polarimeter *in situ*. The circular polarization η_2 is proportional to P, and the polarimeter's analyzing power A, a dynamical energy-dependent quantity, is given by η_3. Finally, if either resonances or spin-orbit forces are important, or if i is not a Russell-Saunders state, the linear polarization fraction η_1 will be nonzero and γ and β cannot be calculated simply [9]. (A particularly vivid example of this is seen with Hg [4].) Thus in cascade-free regions of E, measurement of η_1 serves as a check of the validity of Eq. (1).

We have recently completed a study of polarized electron scattering by the heavy noble gases Ne, Ar, Kr, and Xe, with the goal of searching for evidence of spin-orbit forces acting on the continuum electron [11]. To do this, we measured values of η_1 for light emitted by the $np^5(n+1)p\ ^3D_3$ Russell-Saunders states. (Of all the states in the $np^6(n+1)p$ manifold, only the $^3D_3$ state is a pure triplet with good LS coupling. The others exhibit varying levels of intermediate coupling, i.e., do not have well-defined values of L and S [9].) Nonzero η_1 values, which we failed to find, would have been a clean signature of such forces. In the course of this work, however, it dawned on us that the transitions we were studying represented ideal candidates for optical electron polarimetry.

In Table I, we list some characteristics of the relevant transitions for the $^3D_3$ states in the heavy noble gases we studied as well as the polarimetric $3\,^3P-2\,^3S$ transition in He. Four potential advantages of the heavy noble gas transitions are apparent. Their peak optical excitation cross sections and threshold analyzing powers are larger than those of He, meaning that for a given electron input current and polarization, the fluorescence will be brighter and more polarized with heavy noble gas targets. Moreover, A for the heavy noble gases is enhanced by collisionally produced alignment (given by η_3) instead of being reduced as it is with He. (Values of η_3 are positive for all transitions and energies considered here.) Finally, the gap between the initial-state threshold energy E_t and the first cascade threshold E_c are bigger for Ne, Ar, and Kr than for He. This gap can be important because very precise measurements must be made at or below E_c. If gap is small, the effective polarimetric cross section is correspondingly small because of its proximity to the null threshold cross section. Moreover, a larger gap is useful because electron beams with wider energy profiles can be analyzed entirely in the ''safe'' range between E_t and E_c. Thus Ne is significantly better than He in this regard, but Xe is worse. All of these factors contribute to the polarimeter operating efficiency, which will be defined and discussed below.

A final advantage of the heavy noble gases is illustrated in Figs. 1 and 2. The ultimate accuracy of an optical polarimeter is determined in part by how accurately the analyzing power A, or, equivalently, η_3, can be measured. In the case of He, η_3 varies rapidly with energy just above threshold. (Several conjectures for this behavior have been advanced [18–20].) Thus, with He, the measured value of P depends sensitively on the energy profile of the incident beam. In contrast, η_3 for the $np^5(n+1)p\ ^3D_3 \rightarrow np^5(n+1)s\ ^3P_2$ transitions in all the heavy noble gases varies slowly with E [9], so the prospects for accurate measurements of A are better in these systems. This advantage is enhanced both by the fact that He has the only negative β in Table I, and that it has the largest magnitude.

The heavy noble gases have at least two disadvantages as polarimetry targets. Neon, Kr, and Xe are much more expensive than He. More important, however, are the potential effects of negative-ion resonances on γ and β. In He, typical resonance lifetimes ($\sim10^{-14}$ s [21]) are much shorter than the fine-structure relaxation times (corresponding to the splittings between the fine-structure levels) for the $n=3$ manifold ($\sim10^{-11}$ s). In the heavy noble gases, however, most resonance lifetimes ($\sim10^{-14}$ s [21]) are comparable to or longer than the $np^5(n+1)p$ manifold fine-structure periods. Thus, if resonances occur in these systems at energies where the

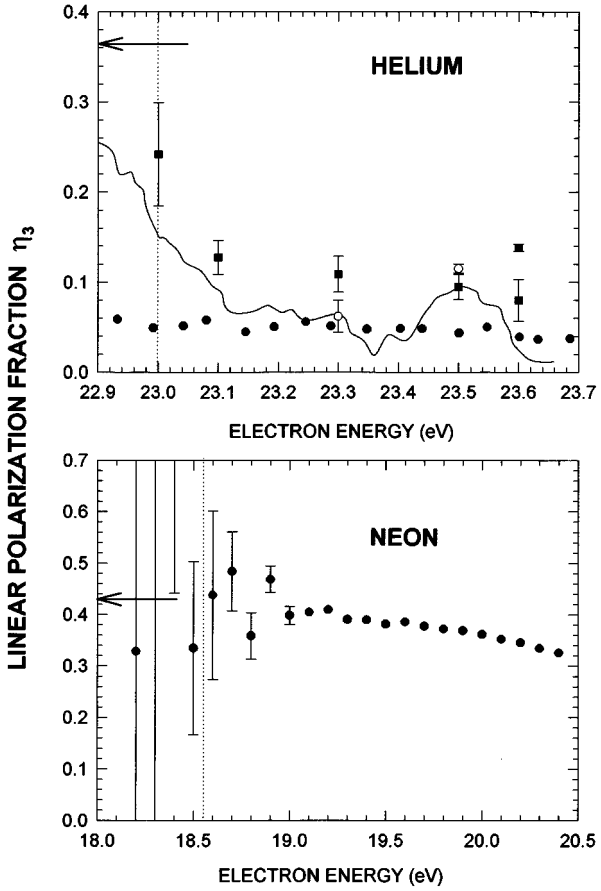

FIG. 2. Linear polarization fraction η_3 of the $3^3P \rightarrow 2^3S$ (3889 Å) transition in He, and the $3p\ ^3D_3 \rightarrow 3s\ ^3P_2$ (6402 Å) transition in Ne, near their excitation thresholds. Horizontal arrows indicate the kinematically required threshold value of η_3; vertical dotted lines indicate the excitation threshold energies. The He data include those of Refs. [6] (solid circles), [8] (open circles), and [17] (solid line), as well as those of this work (solid squares; see also Ref. [7]). Neon data are from this work and that of Ref. [9]. In the cases of Refs. [6] and [17], data below the indicated excitation thresholds are due to the different criteria used to designate the onset energy of signal above background, causing an effective lowering of the energy scale by ~0.1 eV for these data. Our data for Ne below threshold essentially indicate the residual background polarization, and are all within 2 standard deviations of zero.

measurements are made, significant departures of γ and β from their kinematic values could, in principle, occur.

In Sec. II, we discuss the experimental apparatus we used to make these measurements and the procedures we followed. Section III presents our results and conclusions.

II. APPARATUS AND PROCEDURES

The apparatus we used in these experiments has been described at length in three previous reports [7,9,22], and is shown schematically in Fig. 1. A GaAs source produces a beam of transversely polarized electrons (with momentum along $\hat{\mathbf{z}}$ and polarization along $\hat{\mathbf{x}}$), whose polarization is analyzed by a concentric-cylinder Mott polarimeter. The electron beam subsequently traverses a longitudinal B field that rotates the spin direction to $\hat{y}$. In the target chamber, the beam is decelerated from its transport energy of 2 keV to energies below 200 eV, and crosses a multicapillary-array effusive gas target before being collected in a Faraday cup.

Light emitted from the target region along $\hat{y}$ is collected by a borosilicate lens with an acceptance half-angle of 9° and a nominal focal length of 120 mm. This lens is part of the target chamber vacuum wall. The light then passes through several circular apertures 3.8 cm in diameter, a dichroic film polarizer, a retardation plate, and a narrow-band interference filter before being refocused onto the GaAs photocathode of a single-photon-counting photomultiplier tube (PMT).

In these studies, we measured optical excitation functions for the transitions in question, as well as the relative integrated Stokes parameters. Excitation functions were measured between threshold and 100 eV for all five gases, with photon count rates normalized to incident beam current and the target number density n. The value of n was inferred from knowledge of the stagnation pressure behind the effusive multicapillary array using the model discussed by Lucas [23]. The pressure was measured with a capacitance manometer. At each energy, the electron beam was tuned to maximize the photon signal. One beam tuning was usually sufficient for the energy range from threshold to about 5 eV above threshold, and tuning was adjusted at each energy above this. By adjusting beam focusing, we also demonstrated that the entire incident electron current was being collected in the Faraday cup. We also checked that the fluorescence yield was proportional to target gas pressure and, by placing neutral density filters in the GaAs source laser beam, to incident electron current. The use of neutral density filters allowed us to attenuate the electron beam without changing its spatial profile. Excitation function measurements were made with the retarder removed from the optical train and with the linear polarizer transmission axis placed at a 35.2° angle relative to the electron-beam direction. This latter procedure was used to eliminate the effect of excited-state alignment on the fluorescence yield [20,24]. After these data were taken (and the apparatus disassembled), we learned that the correct polarizer angle is 54.8° [24]. Thus the excitation functions reported here have some residual polarization dependence. This effect is relatively small, however, and can be calculated from knowledge of η_3 (see Fig. 9 of Ref. [9]). For all four targets, η_3 drops below 0.2 within 4.5 eV of threshold, so that the ''true'' intensity is at most 12% greater than we measured. The worst case is at threshold, where the intensities we observed are approximately 24% below their polarization-independent value. In any case, the energy-dependent corrections to the excitation functions for each target are very similar because their respective η_3 curves are so much alike.

A number of systematic checks were made of the integrated Stokes parameter measurements. The linear polarization η_3 was determined in a number of cases using two different methods. The first involved the simple rotation of the linear polarizer, which was followed by and attached to the quarter-wave plate, with its fast axis at 45° relative to the polarizer's transmission axis. The quarter-wave plate thus minimized linear instrumental polarization due to the remaining downstream optical elements, including the PMT. In the second, more standard method, the retarder was rotated upstream of the fixed polarizer. Both methods yielded the

same values of η_3 in all cases studied.

Overall linear instrumental polarization of the optical train was studied using an unpolarized light source, consisting of incandescent light sent through an optical fiber bundle, followed by two disks of opal glass. This source was placed at the center of the electron-gas interaction region, and emitted light with an approximate cos θ distribution about $\hat{y}$. The light source in this configuration was axially symmetric about $\hat{y}$, and could be rotated about this axis. By systematic rotation of the source and all elements (including lenses) of the optical train, we concluded that both η_1 and η_3 instrumental asymmetries were at a level below 0.005. Instrumental asymmetries associated with η_2 and η_1 were eliminated by optical flipping of the electron spins at their source.

Other systematic polarization checks included variation of collimating aperture diameters in the optical train, tests of the polarization dependence on target pressure, optical train axis variation, and changing of electron-beam focusing and steering. All of these tests indicated systematic effects below 0.005. Corrections to the Stokes parameters for finite-solid-angle acceptance of the optical train were about 0.008, and were uncertain by 0.001. Background corrections were small in most cases and have been discussed in detail in Ref. [9].

Two polarizers were used for wavelengths above and below 650 nm, respectively. An achromatic polymer sheet retarder was used for all the heavy noble gases, while a zeroth-order quartz waveplate was used for He. The largest uncertainties in the Stokes parameters were due to uncertainty in the optical constants of these elements. The optical constants (the position of the transmission axis and the polarizing efficiency of the polarizers; the position of the fast axis and the retardance of the retarders) were measured at each wavelength using collimated white light with a beam diameter of about 3 cm, equivalent to the beam in the optical polarimeter, passed through the appropriate optical filter. We generally measured values significantly different than those quoted by the manufacturers for all quantities except the positions of the polarizer transmission axes and the zeroth-order quartz retarder fast axis. The most serious discrepancy occurred in the position of the achromatic retarder fast axis, which we measured, using two independent methods [25,26], to be $7°\pm2°$ off that quoted by the manufacturer. Unfortunately, we had made all our polarization measurements referenced to the quoted fast axis, so a $\sim$5% correction had to be made to these data. The causes of these discrepancies are unclear, but they may be due in part to the fact that the measurements of optical constants made by the manufacturers were done with narrow beams, whereas our measurements represent an average over most of the respective elements.

As a check on our optical measurements of P, we also made Mott polarization measurements (see Sec. III). The configuration of our apparatus allowed us to make these measurements simultaneously. The transmission through the Mott polarimeter, however, was severely dependent on the high voltage placed on its inner cylinder, and this limited us to Mott analyzing energies below 25 keV when simultaneous optical measurements were made. Mott measurements were made as described in Ref. [22].

III. RESULTS AND DISCUSSION

Electron polarimeters may be characterized and compared by using a parameter called the ''figure of merit'' Σ, which is inversely proportional to the square of the time required to make a measurement of P to a given statistical uncertainty [27]. All other factors being equal, the larger Σ, the better the polarimeter. The definition of Σ, including its general incident energy dependence, is

$$\Sigma(E)\equiv A^2(E)\left(\frac{I_d(E)}{I_i(E)}\right), \tag{2}$$

where I_i is the number of electrons per second entering the polarimeter, and I_d is the detector count rate. The ratio $I_d(E)/I_i(E)$ is sometimes called the polarimeter's ''efficiency,'' $F(E)$. In order to estimate the relative figures of merit of the various noble gas targets, we measured the optical excitation functions $I_d(E)$ of each transition, as well as the Stokes parameters. For a given target, $I_d(E)$ is proportional to $\sigma(E)$, the optical excitation cross section [14]. We now consider two quantities that are each proportional to $\Sigma(E)$ for a given target.

(1) The ''ideal'' figure of merit, $\Sigma_i(E)$. This quantity, which is independent of apparatus-specific parameters, is defined as

$$\Sigma_i(E)\equiv A^2(E)\sigma(E). \tag{3}$$

It thus provides a basis for evaluating the intrinsic relative merit of various transitions as candidates for polarimetry.

(2) The ''practical'' figure of merit, $\Sigma_p(E)$. For a given apparatus, $\Sigma(E)$ will depend upon a variety of factors including PMT efficiency, solid angle subtended by the optical train, transport efficiency of the electron-optical input elements, and the transmission of the optical interference filter used to isolate the transition in question. In order to provide an example of how actual polarimetric figures of merit can vary from target to target for a given apparatus, for our measurements we define

$$\Sigma_p(E)\equiv A^2(E)F(E)/n. \tag{4}$$

Thus Σ_p is essentially a target-density-normalized version of Σ. As mentioned above, n for our experiment is calculated using the model of Lucas [23] and the target stagnation pressure above the effusive source. While we expect that our knowledge of n using this method will not be accurate to better than a factor of 2 or 3 for a given gas, relative densities needed for the comparison of Σ_p for two targets should be known considerably better than this.

Our measurements of $I_d(E)$, proportional to the optical excitation cross sections, are shown in Fig. 3. They have been normalized at their maximum values to the absolute optical peak cross sections of Refs. [13–16]. The normalization was done at the peak values because relative statistical errors are least there, as are possible pressure-dependent effects [28]. Several other excitation function measurements, also normalized, where necessary, to the peak cross sections are shown in these figures for comparison.

In order to calculate $\Sigma_i(E)$ and $\Sigma_p(E)$, the functions $A(E)$ were obtained using the calculations and data of Refs. [8] and [9]. We take $A(E)$ to be the kinematically required threshold value of the analyzing power $A(E_t)$, times the ratio $\eta_2(E)/\eta_2(E_t)$. The various values of $A(E_t)$, listed in Table I, take into account the hyperfine depolarization and isotopic

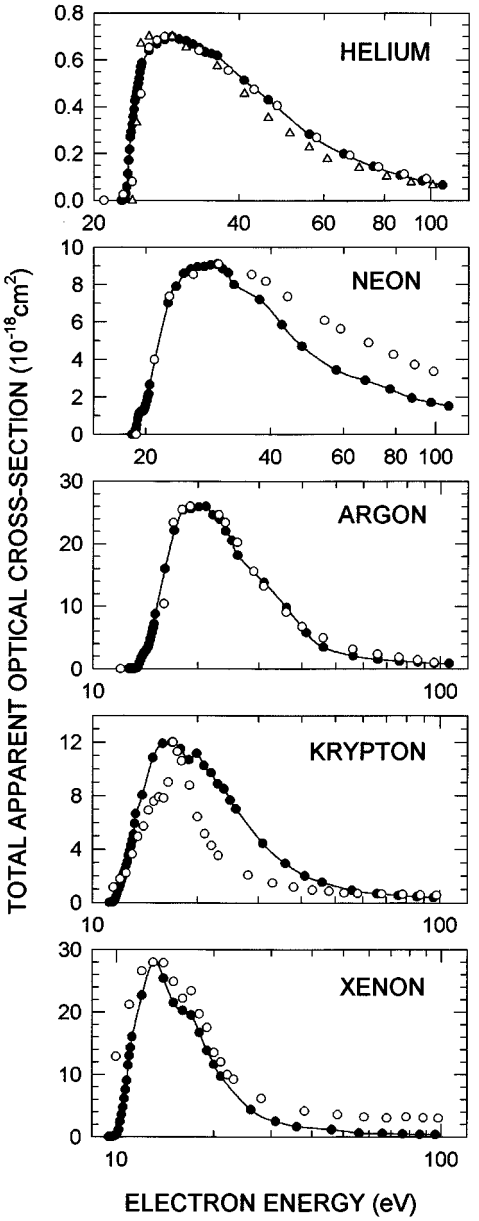

FIG. 3. Optical cross sections for the polarimetric transitions, obtained by normalization of the peak counting rates to the maximum absolute apparent optical cross sections ($\sigma_{\max}$) listed in Table I. Shown also are the optical cross sections of Refs. [28] (triangles) and [29] (open circles) for He, both normalized to the peak value of Ref. [13]; Ref. [14] (open circles) for Ne; Ref. [15] (open circles) for Ar; and Ref. [16] (open circles) for Kr and Xe. The Xe and Kr data of Ref. [16] have been extrapolated to zero target pressure. Data sets have been shifted in energy to provide the best matching of energy-dependent features.

makeup of each target and assume that at threshold, only states with $m_l=0$ are excited [9]. Combining $A(E)$ and $\sigma(E)$ [obtained by normalizing our measured values of $I_d(E)$ to the peak optical cross sections] yields $\Sigma_i(E)$ for each gas. These results are shown in Fig. 4. Inspection of this figure confirms our initial contention that the heavy noble gases are superior to helium as polarimetric targets; figures of merit for neon, the least efficient heavy noble gas target, are 20–30 times those of He at the same incident electron energies.

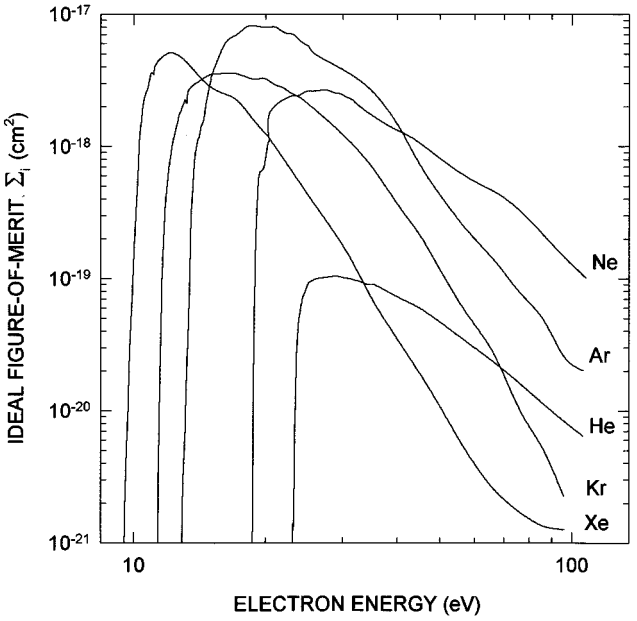

FIG. 4. Ideal figures of merit for the various polarimetric transitions.

The polarimeter constants γ and β can be calculated algebraically only below E_c. Thus the most accurate measurements of P (i.e., those not requiring calibration) should be made at E_c. In Table II, we have listed $\Sigma_i(E_c)$ and $\Sigma_p(E_c)$ for the various gases normalized to He values of unity. We note that $\Sigma_i(E_c)$ for Xe is relatively low compared to the other heavy noble gases. This is because of its small gap between E_t and E_c. We compare also the maximum values of Σ_i and Σ_p relative to the He cascade values in Table II. Measurements of P at the energies corresponding to these maxima would require calibration, but this can be done *in situ* simply by measuring the ratio $\eta_2(E_{\max})/\eta_2(E_c)$, where $E_{\max}$ is the energy at which the maximum value of Σ_p (or Σ_i) occurs.

The largest value of $\Sigma_i(E_{\max})$ we find is for argon: 8.2×10^{-18} cm^2. This number can be used to estimate the maximum practical figure of merit that can be realized with optical polarimeters. Our effusive target had an effective areal density nl of about 10^{11} cm^{-2}, with l being defined essentially by the overlap of the electron beam and the field of view of the optical train. The nl product could easily be increased to $\sim10^{14}$ by using a static gas target cell without danger of radiation trapping [28]. Taking an optical solid angle of 8×10^{-2} sr and a transmission/detection efficiency of 0.03 for the optical train (our apparatus values) yields a best-case figure of merit with argon of 1.5×10^{-7}.

TABLE II. Relative polarimetric figures of merit.

Target	$\Sigma_i(E_c)$	$\Sigma_i(E_{\max})$	$\Sigma_p(E_c)$	$\Sigma_p(E_{\max})$
He	1	9	1	9
Ne	59	232	17	65
Ar	87	709	19	154
Kr	84	312	137	510
Xe	13	443	203	7130

TABLE III. Values of the linear polarization fraction η_1 measured at the first cascade threshold energy E_c.

Target	$\eta_1(E_c)$
He	0.0009(11)
Ne	−0.0002(12)
Ar	−0.0021(35)
Kr	0.0037(48)
Xe	0.0049(85)

With hard work, this number might be increased, but it is fair to say that a practical upper limit on Σ for optical polarimeters is 5×10^{-7}. Herein lies the chief disadvantage of the optical technique. Mott polarimeters typically have between two and three orders of magnitude larger values of Σ [30].

As discussed above, the validity of Eq. (1) at energies below E_c can be checked by measuring η_1. We have made these measurements for all the transitions studied at their respective values of E_c; the results are listed in Table III. Precision measurements of Stokes parameters close to threshold are difficult because of the low excitation cross sections. These results typically required about 10 h of data accumulation for each transition. We were particularly interested in checking the validity of Eq. (1) for He, where assumptions of LS-coupling and the neglect of resonances and spin-orbit effects are expected to be the most justified. Data were taken for more than 60 h in this case [7]. For all targets, including Xe, where relativistic effects would be expected to be the largest, η_1 is consistent with zero. We find this to be surprising, given that typical negative ion resonances in the heavy noble gases should live significantly longer than their corresponding fine-structure oscillatory periods. In Ne, we observe a prominent resonance in the optical excitation function in immediate proximity to E_c [$2p^5(4s^2,3d^2)$? [21]], but no corresponding effect in any of the Stokes parameters. This means that over the energy range of our measurements, i.e., between the specified energy minus the width of the incident beam (about 0.2 eV) and the energy itself, resonance and spin-orbit effects are negligible at our level of statistical accuracy. Thus polarimetric measurements can be made using these transitions with this level of accuracy or better at these energies, assuming comparable incident electron energy profiles.

As a second check on the accuracy of Eq. (1) for the heavy noble gases, we compared η_2 measurements using targets of He and Kr to simultaneous Mott scattering asymmetry measurements. [Krypton was used because of its large value of $\Sigma_p(E_c)$ relative to Ne and Ar. Xenon was too expensive.] The electron beam first passed through the Mott polarimeter at 20 keV, where an asymmetry $A_{\rm Mott}$ was determined after proper background subtraction [22]. 200-Å-thick gold films backed by Formvar were used as Mott scattering targets, and electrons which had lost up to 300 eV in the target were detected. The asymmetry $A_{\rm Mott}$ is given by $PS_{\rm eff}$, where $S_{\rm eff}$ is the ''effective Sherman function'' (or analyzing power) of the device [30]. Subsequently, after 90° spin rotation (Fig. 1), the optical polarimeter measured $\eta_2=A(E_c)P$. Thus either Kr or He measurements could be used to determine $S_{\rm eff}$ for the Mott polarimeter, since η_3 and η_2 are measured, and γ and β are exactly calculable at E_c:

$$S_{\rm eff}=\frac{A_{\rm Mott}}{P}=\frac{A(E_c)}{\eta_2(E_c)}. \tag{5}$$

Agreement between the values of $S_{\rm eff}$ measured with Kr and He constitutes *circumstantial* evidence for the validity of Eq. (1) for both targets; it is unlikely that relativistic effects would cause the breakdown of Eq. (1) for both targets in such a way that the individual deviations would lead serendipitously to agreement between the two $S_{\rm eff}$ results. Using He, $S_{\rm eff}$ was measured to be $0.1478\pm0.0012\pm0.0012$, where the first uncertainty is due to counting statistics, and the second is a systematic uncertainty resulting from the measurements of η_3 and the optical constants of the polarizing elements. With Kr, we obtain $S_{\rm eff}=0.1434\pm0.0007\pm0.0039$. These numbers differ by 3.0%, and essentially agree with each other at the level of one standard deviation of the combined uncertainties.

We believe that with a more thorough analysis and characterization of our optical polarimeter, the systematic uncertainties associated with Stokes parameter measurements can be pushed below the level of 0.5% of the polarization value. Also, replacement of the effusive target with a static gas cell would increase the target areal density by at least two orders of magnitude, meaning that uncertainties due to counting statistics should be reduced by an order of magnitude. For this reason, we believe that ultimate limits on the accuracy with which such measurements can be made will be imposed by the optical polarimetry, as well as other potential systematic effects associated with, e.g., negative-ion resonances, magnetic fields (causing precession of the excited target states), spurious backgrounds, especially from other atomic transitions, and possible energy dependence of P within the incident-electron-beam width [31].

IV. SUMMARY

This work has demonstrated the superiority of the heavy noble gases to helium as targets for optical electron polarimetry. The heavy noble gases have three major advantages: larger overall excitation cross sections, larger analyzing powers, and (with the exception of Xe) larger gaps between the threshold energy for excitation and the threshold energy for production of the first cascading states. These factors cause the heavy noble gas targets to have figures of merit between one and two orders of magnitude larger than those of He. Moreover, we have shown that at a level of better than 0.01 (Table III), the heavy noble gases appear to be unaffected by spin-orbit or resonance effects at the energy where the most accurate measurement of P can be made without calibration, E_c. Our studies comparing He and Kr transitions using the Mott polarimeter corroborate this at a level of accuracy better than 0.004.

It is clear that further improvements in the accuracy of this technique will occur primarily as a result of improved optical polarimetry. It is our hope that in the future, we will be able to make Stokes parameter measurements to better than 0.5% of the polarization value. At this level, deviations from Eq. (1) due to resonances and spin-orbit effects may become observable, especially given the fact that resonance lifetimes are comparable to or longer than the fine-structure oscillatory periods of these systems. Another potential prob-

lem for the optical technique at this level would arise from trying to characterize certain types of GaAs sources whose beams have a strong energy dependence of P within the beam energy profile [31]. In these cases, the strong energy dependence of $I_d(E)$ near threshold would have to be taken into account to extract an average value of P.

Future work in our lab will concentrate on improving the optical polarimetry required by these analyzers and the development of devices that can be used in a variety of experiments and configurations.

ACKNOWLEDGMENTS

The authors would like to thank J. D. Clark of Wright State University for communicating to us excitation function data from his group on Xe and Kr prior to publication. J. Abdallah of Los Alamos National Laboratory and S. J. Buckman of the Australian National University provided us with useful information at critical junctures. This work was supported by NSF Grant No. PHY-9504350, and the Universities of Nebraska and Missouri.

[1] E. S. Dayhoff, quoted as a private communication by H. A. Tolhoek, Rev. Mod. Phys. **28**, 277 (1956).

[2] P. S. Farago and J. S. Wykes, J. Phys. B **2**, 747 (1969); J. S. Wykes, *ibid*. **4**, L91 (1971).

[3] M. Eminyan and G. Lampel, Phys. Rev. Lett. **45**, 1171 (1980).

[4] A. Wolcke, K. Bartschat, K. Blum, H. Borgmann, G. F. Hanne, and J. Kessler, J. Phys. B **16**, 639 (1983).

[5] T. J. Gay, J. Phys. B **16**, L553 (1983).

[6] J. Goeke, G. F. Hanne, and J. Kessler, Phys. Rev. Lett. **61**, 58 (1988); M. Uhrig, A. Beck, J. Goeke, F. Eschen, M. Sohn, G. F. Hanne, K. Jost, and J. Kessler, Rev. Sci. Instrum. **60**, 872 (1989).

[7] T. J. Gay, J. E. Furst, H. Geesmann, M. A. Khakoo, D. H. Madison, and W. M. K. P. Wijayaratna, in *Correlations and Polarization in Electronic and Atomic Collisions and (e,2e) Reactions*, edited by P. J. O. Teubner and E. Weigold, IOP Conf. Proc. No. 122 (Institute of Physics and Physical Society, Bristol, 1992), p. 265.

[8] I. Humphrey, C. Ranganathaiah, J. L. Robbins, J. F. Williams, R. A. Anderson, and W. C. Macklin, Meas. Sci. Technol. **3**, 884 (1992).

[9] J. E. Furst, W. M. K. P. Wijayaratna, D. H. Madison, and T. J. Gay, Phys. Rev. A **47**, 3775 (1993).

[10] K. Bartschat and K. Blum, Z. Phys. A **304**, 85 (1982).

[11] J. E. Furst, T. J. Gay, W. M. K. P. Wijayaratna, K. Bartschat, H. Geesmann, M. A. Khakoo, and D. H. Madison, J. Phys. B **25**, 1089 (1992).

[12] J. Reader, C. H. Corliss, W. L. Wiese, and G. A. Martin, *Wavelengths and Transition Probabilities for Atoms and Atomic Ions*, NBS Document No. 248-B (U.S. General Printing Office, Washington, D.C. 1981).

[13] A. F. J. van Raan, J. P. de Jongh, J. van Eck, and H. G. M. Heideman, Physica **53**, 45 (1971).

[14] F. A. Sharpton, R. M. St. John, C. C. Lin, and F. E. Fajen, Phys. Rev. A **2**, 1305 (1970).

[15] J. K. Ballou, C. C. Lin, and F. E. Fajen, Phys. Rev. A **8**, 1797 (1973).

[16] J. D. Clark, K. Rimkus, and C. A. DeJoseph, Jr. (private communication).

[17] D. W. O. Heddle, R. G. W. Keesing, and A. Parkin, Proc. R. Soc. London Ser. A **352**, 419 (1977).

[18] H. Hafner, H. Kleinpoppen, and H. Krüger, Phys. Lett. **18**, 270 (1965).

[19] R. H. McFarland and M. H. Mittleman, Phys. Rev. Lett. **20**, 899 (1968).

[20] U. Fano and J. H. Macek, Rev. Mod. Phys. **45**, 553 (1973).

[21] S. J. Buckman and C. W. Clark, Rev. Mod. Phys. **66**, 539 (1994).

[22] T. J. Gay, M. A. Khakoo, J. A. Brand, J. E. Furst, W. V. Meyer, W. M. K. P. Wijayaratna, and F. B. Dunning, Rev. Sci. Instrum. **63**, 114 (1992).

[23] C. B. Lucas, Vacuum **23**, 395 (1973).

[24] B. L. Moiseiwitsch and S. J. Smith, Rev. Mod. Phys. **40**, 238 (1968), who cite Burrows and Dunn. This reference states that the pass axis of the polarizer should be placed at 35.2° to the electron beam. A more recent reference, P. N. Clout and D. W. O. Heddle, J. Opt. Soc. Am. **59**, 715 (1969), which we believe to be correct, shows the angle to be 54.8°. Unfortunately, all our data were taken with the former angle. This means that our intensity measurements have some residual polarization dependence.

[25] H. G. Berry, G. Gabrielse, and A. E. Livingston, Appl. Opt. **16**, 3200 (1977).

[26] R. L. Brooks and E. H. Pinnington, Phys. Rev. A **18**, 1454 (1978); R. L. Brooks, Ph.D. Thesis, University of Alberta (Edmonton), 1978 (unpublished).

[27] J. Kessler, *Polarized Electrons*, 2nd ed. (Springer, Berlin, 1985), p. 242.

[28] D. W. O. Heddle and C. B. Lucas, Proc. R. Soc. London Ser. A **271**, 129 (1962).

[29] R. H. McFarland and E. A. Soltysik, Phys. Rev. **127**, 2090 (1962).

[30] T. J. Gay and F. B. Dunning, Rev. Sci. Instrum. **63**, 1635 (1992).

[31] H.-J. Drouhin, C. Hermann, and G. Lampel, Phys. Rev. B **31**, 3872 (1985).